In Table 2, the proposed method is compared with the CLT, the high-order shear deformation theory (HSDT),[2] and the three dimensional elasticity solution given in Ref. 3, for $R/H = 2, 5, 10, 20,$ and 100. It is seen that CLT is reasonably accurate only when $R/H \geq 20$, whereas HSDT is good for $R/H \geq 10$. The proposed method is valid for all of the R/H values and gives predictions that are in agreement with those of Ref. 3.

As a second example, cross-ply, orthotropically laminated cylindrical shells are modeled. The thickness of every layer is the same: $h_k = H/NL$. The laminating sequence, which starts with the first (inner) layer, is 90/0/90..., where 90 deg means that the fibers are aligned with the θ direction and 0 deg the x direction. The shell is subject to the patch load shown in Fig. 1. The width and subtended angle of the load are taken as $L_p = L/4$ and $\theta_p = \pi/8$.

The proposed three-dimensional elasticity theory is compared with the CLT and the HSDT. Figure 2 shows the distributions of the stresses $\bar{\sigma}_x$ and $\bar{\sigma}_\theta$ of a two-layered shell along the radial direction. Because the shell is thin ($R/H = 10$), the predictions by these theories have small deviations. However, when the shell is relatively thick, say $R/H = 5$, CLT and HSDT lead to large errors, as shown in Figs. 3 and 4 where the stress distributions of a two-layered shell and a five-layered shell are plotted. Apparently, in this case, three-dimensional elasticity theories have to be utilized.

Concluding Remarks

The proposed method is highly accurate in predicting the three-dimensional stresses and displacements of composite shells with arbitrary thickness. One advantage of the method is that various loads and lamina properties are systematically treated by the explicit and compact matrix form of the spatial state-space formulation, which is convenient for computing coding.

For an orthotropic cylindrical shell, the transverse deformation and three-dimensional deformation effects are significant even if the shell is moderately thick. With $L/R = 1$, the classic laminated theory can only be used with reasonable accuracy for $R/H \geq 20$ and higher order shear deformation theory is reliable for $R/H \geq 10$. It is seen that three-dimensional elastic deformation must be taken into consideration even for moderately thick shells, not to mention very thick shells. The proposed method is valid for both thin and thick shells with arbitrary R/H values.

Although this work has focused on SS shells, the proposed method is readily extended to more general boundary conditions. Also, the method can be applied to dynamic problems of laminated shells when combined with the distributed transfer function method.[8]

Acknowledgment

This work was partially supported by the U.S. Army Research Office.

References

[1]Bhaskar, K., and Varadan, T. K., "Benchmark Elasticity Solution for Locally Loaded Laminated Orthotropic Cylindrical Shells," *AIAA Journal*, Vol. 32, No. 3, 1994, pp. 627–632.

[2]Bhimaraddi, A., and Stevens, L. K., "On the Higher Order Theories in the Plates and Shells," *International Journal of Structures*, Vol. 6, No. 1, 1986, pp. 35–50.

[3]Chandrashekhara, K., and Kumar, B. S., "Static Analysis of Thick Laminated Circular Cylindrical Shells," *Journal of Pressure Vessel Technology*, Vol. 115, May 1993, pp. 193–200.

[4]Flugge, W., and Kelkar, V. S., "The Problem of an Elastic Circular Cylinder," *International Journal of Solids and Structures*, Vol. 4, 1968, pp. 397–420.

[5]Fung, Y. C., *Foundations of Solid Mechanics*, Prentice–Hall, Englewood Cliffs, NJ, 1968.

[6]Misovec, A. P., and Kempner, J., "Approximate Elasticity Solution for Orthotropic Cylinder Under Hydrostatic Pressure and Band Load," *Journal of Applied Mechanics*, Vol. 37, No. 1, 1970, pp. 101–108.

[7]Ren. J. G., "Analysis of Simply-Supported Laminated Circular Cylindrical Roofs," *Composite Structures*, Vol. 11, No. 4, 1989, pp. 277–292.

[8]Zhou, J., and Yang, B., "A Distributed Transfer Function Method for Analysis of Cylindrical Shells," *AIAA Journal*, Vol. 33, No. 9, 1995, pp. 1698–1708.

Experimental Investigation on Blade-Stiffened Panel with Stiffener-to-Skin Fiber Stitching

Chen-Wen Chang* and Wen-Bin Young†
National Cheng-Kung University, Tainan 70101, Taiwan, Republic of China

Introduction

ADVANCED composite materials have been used in the aerospace industry because of high strength and low weight. Resin transfer molding (RTM) is believed to be one of the candidates for fabricating advanced composites with lower cost.[1,2] Application of composite materials to aircraft fuselage or wing structures offers potentially significant weight reduction relative to the metallic structures. Stiffened panels are the basic unit of these structures. Traditionally, the stiffened panels have been fabricated by the techniques of adhesive bonding or cocuring of the skin and stiffener components made of prepreg laminates. To reduce the cost, the RTM process could be used to fabricate composite stiffened panels in future aircraft.

For stiffened panel structures, improvement of the damage tolerance is still a major issue for component design. In general, a toughened resin system or three-dimensional textile fiber preform could provide some improvements. However, fiber stitching is found to be an easy and cost-effective method to enhance the properties of the composite in the thickness direction, as compared with conventional laminates. In several studies, through-the-thickness stitching of the fibrous preform was reported to improve damage tolerance and residual strength after impact of the composites.[3–5] For fuselage and wing-box structures, the stiffener-to-skin separation is one of the major considerations of the panel failure as subjected to the internal pressure, either the cabin differential pressure or the wing-box fuel tank pressure. The stiffener and skin may be stitched in an efficient way to enhance the integrity of the panel. This study investigates the reinforcing effect of stiffener-to-skin stitching on flat blade-stiffened composite panels. T-shaped composite parts, which represented a unit of the blade-stiffened panel, with fiber stitching in the joint areas were fabricated. Several types of stitching configurations were tested to evaluate the influence of stitching.

Experimental Design

The mold design consisted of three parts. The upper mold was made of a 41 × 41 × 4.6 cm 6061-T6 aluminum plate. The lower mold included two parts made of 38.1 × 20.5 × 20.2 cm T6061-T6 aluminum blocks. The inlet was located at one corner of the stiffener and two outlets at the corners of the flange. An O-ring seal was used in all of the mating parts to seal the mold and prevent leakage during the resin injection. The T-shaped structure is shown in Fig. 1.

In the RTM process, after mold filling, the mold was kept at a constant temperature for a period of time to cure the specimen. Clamping, which generated the necessary pressure during the filling and curing processes, was provided by an hydraulic press. The press also had a heat source for mold temperature control. Resin was injected into the mold using a pressure vessel connected to a compressed air source. The resin system was CIBA-GEIGY epoxy resin (Araldite LY 564 and Hardener HY 2954), and the reinforcements were made of TGFW-600 woven roving glass fiber mats with 600 g/m^2 surface density. Fiber mats were cut into the desired size and stitched using Kevlar® 49 to form the preform, then stacked into the mold by hand. The diameter of the needle was 1.3 mm,

Received Aug. 1, 1995; revision received Nov. 7, 1995; accepted for publication Dec. 5, 1995.

*Graduate Student, Institute of Aeronautics and Astronautics.
†Associate Professor, Institute of Aeronautics and Astronautics.

Table 1 Thickness and fiber volume contents in each section

	Thickness, mm	No. of layers	Fiber volume content, %
A	5.20	10	45.07
B	4.20	9	50.22
C	3.40	6	41.36

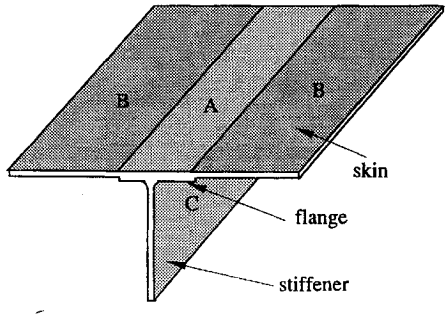

Fig. 1 T-shaped structure.

and lock stitches were used. A constant pitch, 5.3 mm, was used in every specimen. The resulting fiber volume contents of the T-shaped structures are shown in Table 1, where A, B, and C denoted in Fig. 1 represent areas with different thicknesses.

Mold filling process began when the temperature of the entire mold assembly reached a steady value (50°C in this study). The valve near the inlet gate was opened and resin was injected into the mold under a constant pressure using the injecting device. When resin began to flow out of the outlet gate, both valves at the inlet and outlet gates were closed and the mold temperature was raised to 145°C for the curing process. This condition was maintained for about 2 h until the entire part was cured. As the mold cooled down, the part could be demolded.

Number and Location of the Fiber Stitching

In fabrication of integrally stiffened panels, fiber preforms of the skin and stiffener are made separately and stitched together. Studies[4,5] have shown that fiber stitching could effectively increase compression strength after impact and resistance to delamination. As for the assembly of the skin and stiffener, the question is how those components can be stitched together in an efficient way to obtain higher bearing load at the joint as compared with the adhesive bonding. In this study, different T-shaped structures were fabricated with different number and locations of stitching at the stiffener and flange. In group 1, fibers are stitched on the stiffener at 130 (position a), 120 (position b), or 110 (position c) mm from the edge of the stiffener. In group 2, fibers are stitched on the flange at 30 (position a), 20 (position b), or 10 (position c) mm from the edge of the flange, respectively. In group 3, different numbers of Kevlar fibers were used to stitch the stiffener. In group 4, a similar arrangement was made on the flange.

The pull-off test, a similar loading case for a stiffened panel under internal pressure, was conducted to measure the stiffener-to-skin failure load for the panels with different stitching configurations. The stiffened panel was cut into small specimens for test with dimension, $17 \times 2.55 \times 8$ cm. Under a material test system machine, pull-off tests were conducted with a constant displacement (0.25 mm/s) to measure the stiffener-to-skin failure load. The test load was based on the averages of four specimens cut from different panels fabricated under the same conditions.

Table 2 shows the pull-off load at failure as normalized with respect to the length of stiffener. The failure load was defined as the maximum pulling force during the test. Specimens with stitches on either the flange or the stiffener seem to have slightly higher failure pull-off loads than those without stitches. However, because of the data scattering, no sound conclusion could be derived based on these test data. It was suspected that stitches on either the flange or the stiffener alone did not provide much reinforcement effect. From the observation of the failure stages, cracks tended to propagate along the unstitched stiffener as the flange was stitched, or vise versa, and thus reduced the effect of stitching. A selected combination of fiber stitches on both the stiffener and the flange was tested. The failure pull-off load is shown in Fig. 2, where specimen D is made by two stitches on the flange and one stitch on the stiffener close to the root of the stiffener. The stiffener-to-skin failure load of the panel is improved by 25% compared with the case in which no stitches are used.

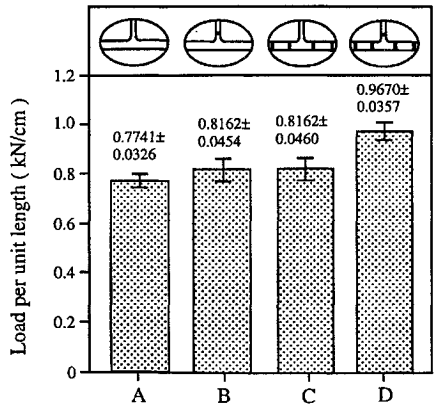

Fig. 2 Normalized failure load for the pull-off test with different stitch configurations.

Pull-Off Load After Impact

The pull-off test after impact was used to assess the damage tolerance of the stiffened panel with a stitched joint. Impact was made on the skin side directly beneath the stiffener with a line impactor under a drop test device. For comparison, specimens without fiber stitches and with different stitching configurations were made. The low-velocity impact energy was 7.35 J for each drop test. Results of the pull-off test after low-velocity impact are shown in Fig. 3. The residual pull-off load of the panel without fiber stitches is only about 23% of the original value. For specimens with fiber stitches, the residual pull-off load was about 70–80% of the original value. Comparison of the specimens A and B indicate that stitching can increase the failure pull-off load of the stiffener-to-skin joint with low-velocity impact damage. For the specimens B and C with different number of fiber stitches, the residual pull-off load after impact for specimen C (two fiber stitches) is slightly higher. In specimen D, fiber stitching on both the stiffener and the flange provides superior property to the stiffened panel, having higher before and after impact pull-off loads.

For stiffened panels subjected to the pull-off test, only 23% of the strength is left after low-velocity impact. With fiber stitches, the retained strength after impact can reach 70–80%. Fiber stitches on the stiffener and flange of the stiffened panel could improve the strength of the stiffener-to-skin joint and the residual strength after impact.

Moderate Velocity Impact

Experimental studies were conducted to investigate the effect of fiber stitching on the damage areas of stiffened panels under moderate velocity ballistic impact. Three configurations were considered: specimens without fiber stitching (configuration 1), specimens with stitches on the flange near the root of the stiffener (configuration 2), and specimens with two stitches on both the stiffener and flange being located away from the root of the stiffener (configuration 3). An air gun with hemisphere impactor head was used in the impacting tests. The impactor was made of DC-53 steel with a length of 38.7 mm, diameter of 12.7 mm, and weight of 36.1 g. A velocity-measuring device made of two infrared units was placed in front of the specimen to measure the oncoming velocity at impact. During all of the tests, the impactor did not totally penetrate the specimen.

Impact was made on the skin side directly beneath the stiffener. Table 3 lists the data on the impact energy and resulting dimensions of the damage zone normalized by the impact energy. It had less damage area for specimens with stitches than without stitches. For

Table 2 Normalized failure load for different stitching configurations

	No stitch[a]	Stitch at position a	Stitch at position b	Stitch at position c
Group 1, one stitch on stiffener	0.7741 ± 0.0326	0.8162 ± 0.0454	0.7851 ± 0.0713	0.7922 ± 0.0689
Group 2, one stitch on flange	0.7741 ± 0.0326	0.7994 ± 0.0573	0.7791 ± 0.0474	0.7275 ± 0.0822
	No stitch	One stitch	Two stitches	Three stitches
Group 3, on stiffener	0.7741 ± 0.0326	0.8162 ± 0.0454	0.8234 ± 0.0352	0.7227 ± 0.0320
Group 4, on flange	0.7741 ± 0.0326	0.7994 ± 0.0573	0.8162 ± 0.0460	0.7182 ± 0.0341

[a]All units in kN/cm.

Table 3 Measured data for moderate velocity ballistic impact

	Stitching configurations		
	1	2	3
Impacting velocity, m/s	102.3	103.1	103.1
Kinetic energy, J	188.90	191.83	191.83
Normalized damage zone, cm^2/J	0.87	0.485	0.665
Depth of damage zone, mm	0.65	1.45	1.9

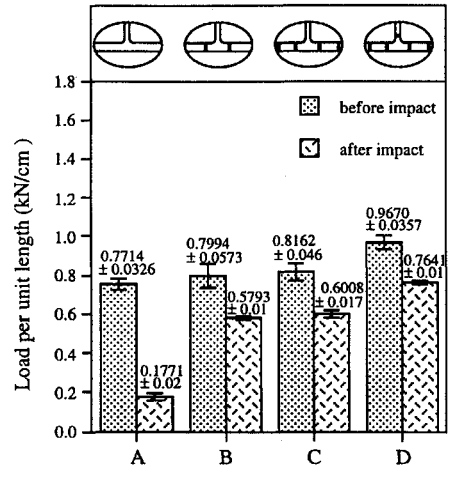

Fig. 3 Normalized failure pull-off load of the stiffened panels before and after impact.

specimens 2 and 3, the stitches of specimen 2 were closer to the stiffener, resulting in less damage area.

Conclusions

For stiffened panels, stitches on both the stiffener and the flange could increase the failure pull-off load by about 25%. As the skin side on the stiffener is subjected to impact, fiber stitches on the stiffener and flange can effectively reduce the crack growth and retain about 70–80% of the original strength of stiffener-to-skin joint.

References

[1]Krolewski, S., and Busch, J., "The Competitive Position of Selected Composite Fabrication Technologies for Automotive Applications," *Proceedings of 35th International SAMPE Symposium*, Society for the Advancement of Material and Process Engineering, 1990, pp. 1761–1771.

[2]Johnson, C. F., Chavka, N. G., and Jeryan, R. A., "Resin Transfer Molding of Complex Automotive Structures," *Proceedings of 41st Annual Conference of SPI*, Session 12-A, Society of the Plastic Industry, New York, 1986, pp. 1–7.

[3]Su, K. B., "Delamination Resistance of Stitched Thermoplastic Matrix Composite Laminates," *Advances in Thermoplastic Matrix Composite Materials*, ASTM STP 1044, American Society for Testing and Materials, Philadelphia, PA, 1989, pp. 279–300.

[4]Mignery, L. A., Tan, T. M., and Sun, C. T., "The Use of Stitching to Suppress Delamination in Laminated Composites," *Delamination and Debonding*, edited by W. S. Johnson, ASTM STP 876, American Society for Testing and Materials, Philadelphia, PA, 1985, pp. 371–385.

[5]Farley, G. L., Smith, B. T., and Maiden, J., "Compression Response of Thick Layer Composite Laminates with Through-the-Thickness Reinforcement," *Journal of Reinforced Plastic and Composites*, Vol. 11, No. 7, 1992, pp. 787–810.

Analytical Model Updating and Model Reduction

R. M. Lin* and M. K. Lim†
Nanyang Technological University, Singapore

I. Introduction

In current vibration practice, structural dynamic characteristics are obtained by using either analytical approaches such as finite element modeling or experimental techniques such as modal testing. However, experience has shown that large discrepancies often exist between analytical predictions and experimental measurements. Under such circumstances, it is generally necessary to correct analytical models in the light of measured data, a process known as model updating.

Various methods to update analytical models using vibration test data have been developed.[1–8] These methods can, in general, be categorized as the reduced-order analytical model approach[1–4] and the full analytical model approach.[5–8] In the former, when the number of measured coordinates is less than the number of degrees of freedom (DOFs) specified in the analytical model, which is usually a case in practice, the analytical model to be updated is usually reduced via model reduction techniques such as the well-known Guyan reduction.[9] In the later, the analytical model is updated in its original full form by either using incomplete vibration test data directly[5–7] or expanding/interpolating unmeasured coordinates based on measured ones.[8] Such an approach is defined here as full analytical model approach, though in practice it is not possible to establish a full model since practical structures possess infinite number of DOFs.[10]

This paper examines the possibilities and limitations of current model updating practice so that further concerted research effort can be made towards more productive direction. It starts with investigating the effect of model reduction on the model updating process and hence demonstrating the practical difficulties associated with reduced-order analytical model updating approach. The advantages and possibilities of full analytical model updating are then discussed and the performance of some recently developed methods examined. Numerical results are given to illustrate the arguments developed.

II. Incompatibility Between Analytical and Experimental Models

In early development of model updating practice, it was always assumed that the number of DOFs specified in an analytical model is

Received Oct. 18, 1995; revision received Nov. 28, 1995; accepted for publication Nov. 29, 1995.

*Lecturer, School of Mechanical and Production Engineering, Nanyang Avenue 2263.

†Associate Professor and Dean, School of Mechanical and Production Engineering, Nanyang Avenue 2263.